COMPARISON OF MAGNETIC RESONANCE IMAGING AND MYELOGRAPHY IN 18 DOBERMAN PINSCHER DOGS WITH CERVICAL SPONDYLOMYELOPATHY

RONALDO C. DA COSTA, JOANE PARENT, HOWARD DOBSON, DAVID HOLMBERG, GARY PARTLOW

Eighteen Doberman pinscher dogs with clinical signs of cervical spondylomyelopathy (wobbler syndrome) underwent cervical myelography and magnetic resonance (MR) imaging. Cervical myelography was performed using iohexol, followed by lateral and ventrodorsal radiographs. Traction myelography was performed using a cervical harness exerting 9 kg of linear traction. MR imaging was performed in sagittal, transverse, and dorsal planes using a 1.5 T magnet with the spine in neutral and traction positions. Three reviewers independently evaluated the myelographic and MR images to determine the most extensive lesion and whether the lesion was static or dynamic. All reviewers agreed with the location of the most extensive lesion on MR images (100%), while the agreement using myelography was 83%. The myelogram and MR imaging findings agreed in the identification of the affected site in 13–16 dogs depending on the reviewer. MR imaging provided additional information on lesion location because it allowed direct examination of the spinal cord diameter and parenchyma. Spinal cord signal changes were seen in 10 dogs. Depending on the reviewer, two to four dogs had their lesions classified as dynamic on myelography but static on MR images. Myelography markedly underscored the severity of the spinal cord compression in two dogs, and failed to identify the cause of the signs in another. The results of this study indicated that, although myelography can identify the location of the lesion in most patients, MR imaging appears to be more accurate in predicting the site, severity, and nature of the spinal cord compression. *Veterinary Radiology & Ultrasound, Vol. 47, No. 6, 2006, pp 523–531.*

Key words: cervical myelopathy, diagnosis, myelogram.

Introduction

CERVICAL SPONDYLOMYELOPATHY, also known as wobbler syndrome, is a common spinal cord disease of large and giant-size dogs.[1] The Doberman pinscher is the breed most commonly affected.[2,3] Myelography has been the diagnostic method of choice for cervical spondylomyelopathy for many years and recent textbooks continue to recommend myelography as diagnostic modality of choice.[4–6] In humans, however, magnetic resonance (MR) imaging is considered the best imaging technique for the evaluation of cervical spondylotic myelopathy.[7,8]

Dynamic or kinematic studies are commonly performed with myelography (traction myelography). These studies allow a distinction between the so-called static and dynamic lesions, considered fundamental for surgical planning.[1,9] Recently, a traction MR imaging technique was described in dogs.[10] Kinematic MR imaging, using flexion, extension, and traction positions, has also been reported in humans.[11–13]

There are several reports comparing myelography and MR imaging in cervical spondylotic myelopathy and other spinal disorders in humans,[14–23] but no reports have been found comparing these imaging modalities in animals. The purposes of this investigation were to compare cervical myelography vs. MR imaging prospectively in Doberman pinscher dogs with clinical signs suggestive of cervical spondylomyelopathy, and to determine how traction MR imaging studies compare with traction myelographic studies in characterizing lesions as static or dynamic.

Material and Methods

Eighteen Doberman pinscher dogs with clinical signs suggestive of cervical spondylomyelopathy were studied prospectively. All dogs were presented to the Small Animal Clinic of the Ontario Veterinary College, University of Guelph, during an 18-month period between June 2003 and November 2004. The investigation was conducted in accordance with the guidelines of and upon approval of the Animal Care Committee of the University of Guelph and the Canadian Council of Animal Care. Physical and

neurologic examinations, complete blood count, and biochemistry profile were performed in all dogs. Eight dogs were tested for von Willebrand's disease using an Enzyme-Linked immunosorbent assay for von Willebrand factor in the plasma. Twelve dogs were tested for hypothyroidism with a panel measuring the serum concentration of total T4, free T4, and thyroid-stimulating hormone. The range of motion of the cervical spine was evaluated by inducing voluntary movements laterally, dorsally, and ventrally, using a food item. The time of onset of clinical signs and the neurologic status of each dog was graded from 1 to 5 (modified from McKee et al.)[24]: Grade 1—cervical hyperesthesia only. Grade 2—mild pelvic limb ataxia/paresis with or without thoracic limb involvement. This degree of ataxia could only be seen after careful gait evaluation. Paw placement was usually consistent throughout most of the evaluation. Grade 3—moderate pelvic limb ataxia/paresis with thoracic limb involvement. This grade was characterized by a consistent and obvious ataxia from the beginning. The dog would often mis-position his pelvic limbs with abduction or adduction often during the gait exam. Grade 4—marked pelvic limb ataxia/paresis with thoracic limb involvement. This ataxia was characterized by a severely abnormal gait, with consistently abnormal foot placement during gait analysis, usually associated with marked pelvic limb weakness. Characteristically, the dogs were lower to the ground in the rear end and would sink as they stood. Grade 5—tetraparesis, unable to stand or walk without assistance.

All dogs had normal cardiac assessment based on electrocardiogram and echocardiography before study enrollment.

Radiographs and myelography were performed under general anesthesia. Survey lateral and ventrodorsal radiographs of the cervical spine were performed, followed by myelography. Cerebellomedullary puncture was performed, allowing cerebrospinal fluid collection and injection of iohexol,* at a dosage of approximately 0.3 ml/kg, attempting to use a maximal volume equal or less than 10 ml per dog. Following injection, the dogs were positioned in sternal recumbency with the head and neck extended for 3–5 min before obtaining lateral and ventrodorsal radiographs of the cervical spine. Thereafter, the linear traction myelographic study was performed using a specially designed harness and 9-kg weight. Lateral radiographs were made during the traction procedure.

For MR imaging, all dogs were anesthetized and positioned in dorsal recumbency. MR imaging was performed using a 1.5 T magnet† and a cervical spine array coil. The field of view was constant for all dogs, at 25 cm in the

sagittal plane and 16 cm in the transverse plane. Two acquisitions (Nex) were obtained for each imaging sequence. A matrix size of 256 × 256 was used for all sections and the slice thickness was 3 mm with no interslice gap for all sequences. The following settings (repetition time [TR] ms, echo time [TE] ms) were used for sagittal images: T1 (TR = 600, TE = 20), turbo spin echo (TSE) T2 (TR = 4620, TE = 120, echo train length = 5), and proton density (PD) (TR = 4620, TE = 20). Images were acquired in the transverse plane using T1, T2, PD, and gradient echo (fast low-angle shot—FLASH–TR = 672, TE = 15, and a flip angle of 30°), combined with magnetization transfer (MT) with and without intravenous gadolinium‡ injection at a dosage of 0.1 mmol/kg. The imaging settings for T1-, T2-, and PD-weighted images were similar to those used in the sagittal plane. The dorsal plane images were acquired with T1-weighted images only. After acquisition of all image sequences with the cervical area in the neutral position, a linear traction study was performed in the same way as described for myelography. The traction study was acquired with sagittal TSE T2-weighted images. The area of imaging extended from the first cervical vertebra (C1) to the second thoracic vertebra (T2). The transverse slices were set parallel to each intervertebral disc and arranged to pass through the center of the discs and the cranial and caudal vertebral end plates. Each intervertebral disc region had five transverse sections, so that for each dog 30 transverse images were obtained in each imaging sequence (T1, T2, PD, gradient echo FLASH, and MT with and without Gd-DTPA), resulting in a total of 150 images of the transverse plane per dog. To avoid variations in image interpretation, all images were printed using a laser film printer at a magnification of 1.25 times. A 5 × 4 format was used for the transverse images and a 4 × 3 format for the sagittal plane images.

Three reviewers analyzed and classified the myelogram and MR images independently. Each reviewer was asked to determine the site of the main lesion(s) and whether the lesion was static or dynamic using nontraction and traction views. Lesions were defined as static when the compression remained upon linear traction, and as dynamic when lesions disappeared upon traction.

On lateral myelography, the site with the most severe extradural compression resulting in the smallest dorsoventral diameter between the dorsal and ventral contrast columns was used to define the main lesion. The same criterion of extradural compression was used for the ventrodorsal myelographic images. The reviewers evaluated both the lateral and ventrodorsal myelographic images in conjunction to determine the location of the main lesion.

The spinal cord region with the smallest dorsoventral or lateral diameter on the sagittal and transverse MR images,

with or without spinal cord signal changes, was considered the main lesion on MR images. When two sites of spinal cord compression were seen on the MR images, the one with spinal cord signal changes was deemed the most important.

Spinal cord signal changes were evaluated on the sagittal T2- and T1-weighted images. Abnormal spinal cord signal changes were classified as hyperintense or hypointense, comparing the area of abnormal signal intensity with the normal spinal cord signal intensity cranial and caudal to the abnormal area. Each intervertebral disc was classified, based on signal intensity changes on T2 mid-sagittal weighted images, as normal, partially degenerated, or completely degenerated. A normal signal was assumed when the disc had a uniform high signal, partial degeneration was assumed when part of the disc had evidence of hypointensity, and total disc degeneration was assumed when the entire disc was hypointense. Foraminal stenosis was evaluated on the gradient echo FLASH with MT post-Gd-DTPA transverse images centered at the disc space. Foraminal stenosis, a narrowing of the intervertebral foramina that may cause compression of the neurovascular structures entering and leaving the spinal cord and vertebral canal, was subjectively classified as absent, mild, moderate, or severe, based on the size and shape of the foramina. The decision as to whether it was normal or stenotic was based on knowledge of the expected normal morphologic appearance at a given level. The presence of abnormal vertebral position (tipping) and spondylosis were evaluated using radiographs and MR images.

Statistical analysis was performed using the κ test to compare the agreement for the location of the main lesion and the lesion characteristic (static or dynamic) on myelogram and MR images among reviewers. The κ test was also used to compare the agreement between myelogram and MR imaging findings regarding the main lesion location and characteristic for each reviewer. Kappa statistics are divided into six categories to determine the closeness of comparisons as follows: poor ($\kappa < 0.10$), slight (0.11–0.20), fair (0.21–0.40), moderate (0.41–0.60), substantial (0.61–0.80), and almost perfect (0.81–1.0).[25] Analyses were performed using the SAS Statistical Software (SAS user's guide. 6th ed. Cary, NC: SAS Institute Inc., 1997).

Results

Ten dogs were male and eight female, and they ranged in age from 3 to 9 years (mean 6 years). Six dogs had an acute onset of clinical signs, 10 dogs a chronic progression of signs, and two dogs had an acute worsening of chronic signs. Neurologically, they were graded as: grade 1, $n = 3$; grade 2, $n = 2$; grade 3, $n = 4$; grade 4, $n = 8$; and grade 5, $n = 1$. Overall, 14 of 18 dogs (77%) had historical or clinical findings of cervical hyperesthesia characterized by a low head carriage, restricted cervical motion, or vocalization upon cervical movement. A thoracic limb posture with elbow abduction and internal rotation of digits ("toe-in posture") was observed in seven dogs. Twelve dogs had asymmetric neurologic deficits, with right-side predominance in nine dogs and left-side predominance in three dogs. Three out of the 12 dogs had markedly asymmetric neurologic deficits. Six out of eight dogs tested were positive for von Willebrand's disease, and eight out of 12 dogs tested were diagnosed with hypothyroidism.

For two reviewers, there was substantial agreement (16/18 dogs, $\kappa = 0.76$) between the myelogram and MR imaging findings regarding the location of the main lesion. For the third reviewer, there was less agreement between the myelogram and MR images, with the main lesion being in the same location in 13 out of 18 dogs, with $\kappa = 0.60$ (moderate agreement). For all three reviewers, the discrepancies occurred in two dogs where the main lesion was located at C5–6 using myelography, but the spinal cord compression associated with signal changes seen on MR imaging indicated that the main lesion was at C6–7 (Fig. 1A–D). For the third reviewer, three other dogs had the main lesion at C4–5 on myelography, but on the MR images the main lesion was identified at C5–6 (two dogs) and C6–7 (one dog).

The κ agreement among the three reviewers using MR images for the location of the main compressive lesion was 100%, with $\kappa = 1.0$. Using myelography, the reviewers agreed in 15 of 18 dogs (83%), with a $\kappa = 0.65$ (substantial agreement).

Most lesions were classified as static on myelography, ranging from 10 to 14 dogs depending on the reviewer, and also as static on MR imaging, ranging from 12 to 16 dogs depending on the reviewer. The most common discrepancy was a lesion classified as dynamic on myelography but static on MR images. This occurred in two to four dogs depending on the reviewer. The three reviewers agreed as to whether the lesion was static or dynamic in 10 out of 18 dogs (56%) using myelography, with $\kappa = 0.33$ (fair agreement), and in 12 out of 18 dogs (67%) using MR imaging, with $\kappa = 0.42$ (moderate agreement). Many dogs with a static lesion had a dynamic component, meaning that the lesion improved but was still present. This was observed in four to 14 dogs using myelography and in four to 13 dogs using MR imaging depending on the reviewer.

In two dogs, the myelogram clearly underestimated the severity of the lesion compared with the MR imaging findings. In one of these dogs, the myelogram gave an impression of a moderate ventrolateral, primarily dynamic, compression, while in the MR images there was a severe circumferential static spinal cord compression with spinal cord atrophy and marked intramedullary signal changes, characterized by hyperintensity and hypointensity in the T2- and T1-weighted images, respectively (Fig. 2A–G). In
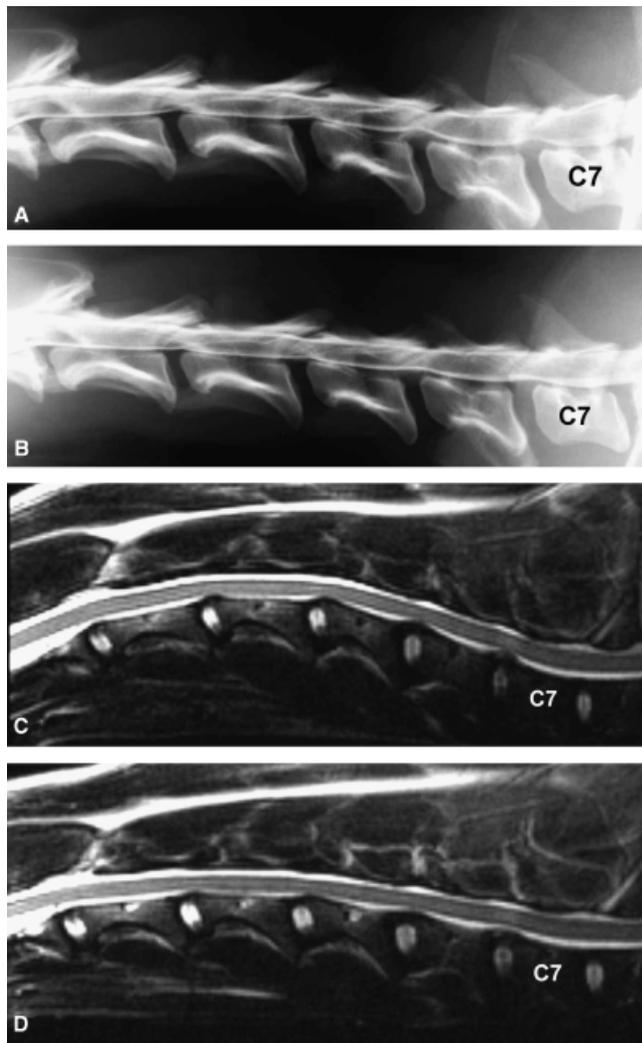
FIG. 1. Cervical myelogram and sagittal T2-weighted images of a 7-year-old, male Doberman pinscher dog with moderate ataxia (grade 3). (A) In the pre-traction cervical myelogram, there is ventral extradural compression at C5–6 and C6–7. The compression at C5–6 was assumed to be the main lesion because of narrowing of the intervertebral disc space and a smaller diameter between the dorsal and ventral aspect of the column of contrast medium. (B) Posttraction cervical myelogram. There is improvement in both compressions, with the lesions being classified as dynamic. (C) Pretraction sagittal T2-weighted image. There is partial intervertebral disc degeneration at C6–7, with spinal cord compression and increased spinal cord signal intensity at the same level. The compression at C6–7 was assumed to be the main lesion based on the spinal cord signal changes. (D) Posttraction sagittal T2-weighted image. There is improvement in the spinal cord compressions. C7, seventh cervical vertebrae.

the other dog, two compression sites were identified using myelography and although one was assumed to be the most important, questions still remained. Using MR imaging, the main spinal cord compression was clearly identifiable and it was possible to appreciate a very asymmetric spinal cord compression not seen on the ventrodorsal myelogram (Fig. 3A–F). Two dogs had a dorsal spinal cord compression that could not be observed on myelog-

raphy, but they were easily identified using MR imaging. Another dog with cervical hyperesthesia only had a partial compression of the subarachnoid space at C5–6 without apparent spinal cord compression on myelography. The MR image findings agreed with the myelogram in this dog not showing spinal cord compression, but revealed disc degeneration and foraminal stenosis at C5–6, which was assumed to be the cause of the clinical signs (based on the absence other MR image changes). In the three dogs with marked asymmetry of clinical signs, the myelogram showed asymmetric cord compression in one, but the compression was found to be contralateral to the main compression on MR images. Asymmetric cord compression was readily observed in the transverse MR images in all three dogs. Two out of these dogs had more severe clinical signs opposite to the side of the main spinal cord compression seen on MR images.

The mean volume of iohexol injected was 10.2 ml (8.5–13 ml) or 0.28 ml/kg. In only three dogs, more than 10.5 ml of iohexol was used. Seizures occurred in five out of 18 dogs (28%) and transient worsening of the neurologic status occurred in six of 18 dogs (33%). The mean contrast volume in the dogs with postmyelographic seizures was 10.0 ml (8.5–12 ml) or 0.28 ml/kg.

Ten out of 18 dogs (55%) had MR imaging signal changes within the spinal cord. All dogs had spinal cord hyperintensity in the T2-weighted images. Two dogs had contrast enhancement in the spinal cord area of abnormal signal intensity after gadolinium injection in the T1-weighted images. Signal changes within the spinal cord were observed in six out of eight dogs with marked ataxia (75%), three out of four dogs with moderate ataxia (75%), and in the dog with nonambulatory tetraparesis. Syringohydromyelia cranial or caudal to the compressive site was seen in two dogs.

Based on the spinal cord signal changes and the smallest spinal cord diameter seen on MR images, the main compressive lesion was found to be at C5–6 in seven dogs and at C6–7 in 10 dogs. One dog with cervical hyperesthesia did not have spinal cord compression but had foraminal stenosis at C5–6. Three dogs had more than one spinal cord compression, one site appearing to be the primary site, with the other(s) less severe. In two out of 18 dogs, the clinical signs were opposite to the side of spinal cord compression.

The cause of the clinical signs was assumed to be associated with disc herniation, with or without concurrent soft tissue or bone changes, in 16 out of the 18 dogs (89%). Foraminal stenosis, and articular process impingement causing bilateral spinal cord compression were assumed as the cause of clinical signs in the other two dogs.

All 18 dogs had intervertebral disc degeneration on MR images. In 16 dogs, it involved multiple discs, while in two dogs it affected only one disc. Disc degeneration was seen more commonly at C6–7 (17 dogs) and C5–6 (15 dogs).
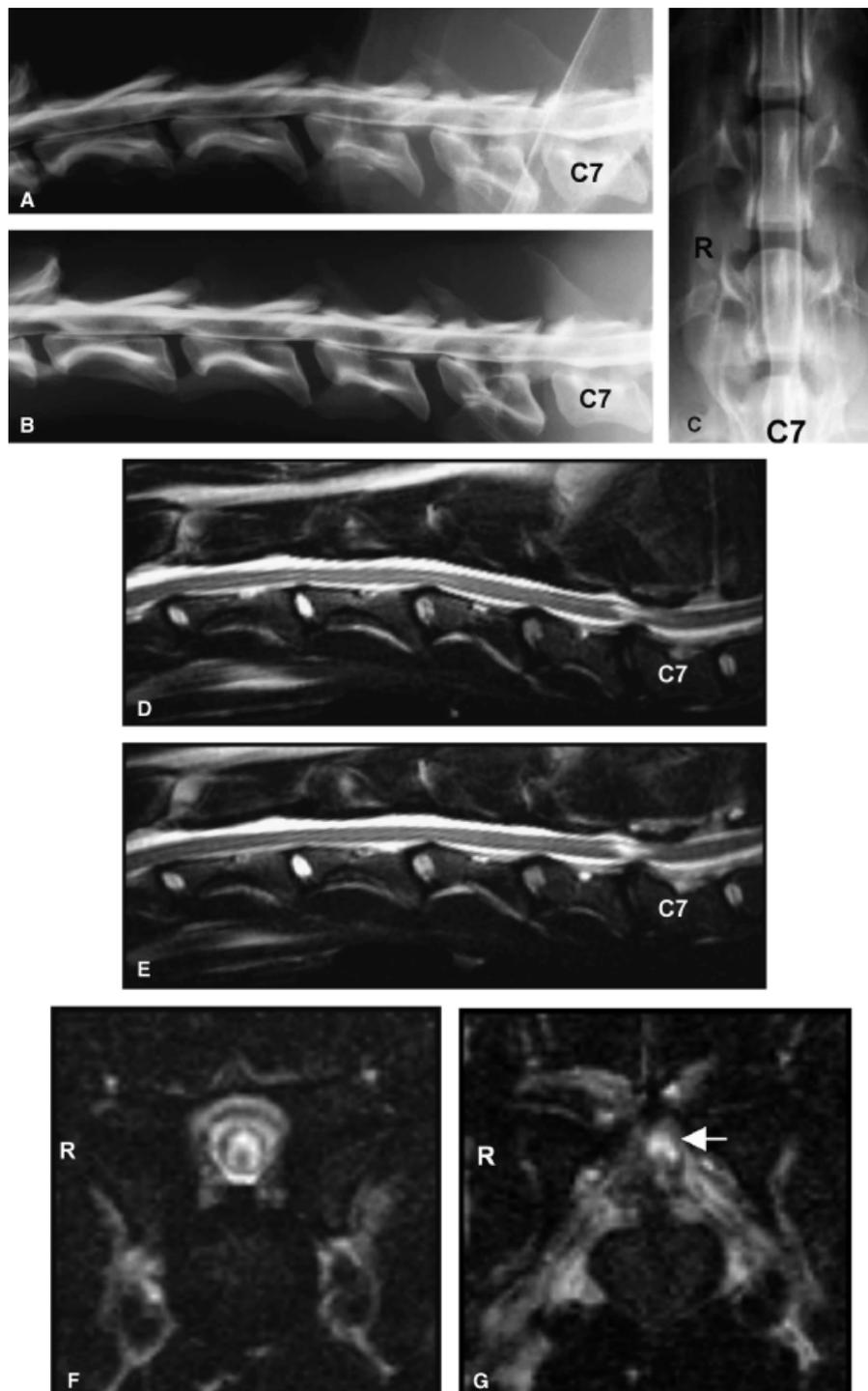
Fig. 2. Cervical myelogram and T2-weighted images of a 7-year-old, neutered male Doberman pinscher dog with severe ataxia (grade 4). (A) Pretraction cervical myelogram. There is ventral extradural spinal cord compression at C6–7. (B) Posttraction cervical myelogram. There is improvement in the ventral compression. Two reviewers classified this lesion as dynamic. (C) Ventrodorsal myelogram. There is bilateral extradural compression worse on the right. (D) Pretraction sagittal T2-weighted image. There is ventral and dorsal spinal cord compression with marked spinal cord hyperintensity at C6–7. Intervertebral disc degeneration is also seen at C6–7. (E) Posttraction sagittal T2-weighted image. There is minimal improvement in the extent of ventral spinal cord compression. All reviewers classified the lesion as static. (F) Transverse T2-weighted image at the cranial region of the spinal cord compression. Note the bilateral spinal cord compression with cord hyperintensity. (G) Transverse T2-weighted image at the central aspect of the cord compression. There is marked circumferential compression and a small, atrophic spinal cord that is seen as an irregular area of hyperintensity (arrow). C7, seventh cervical vertebrae.
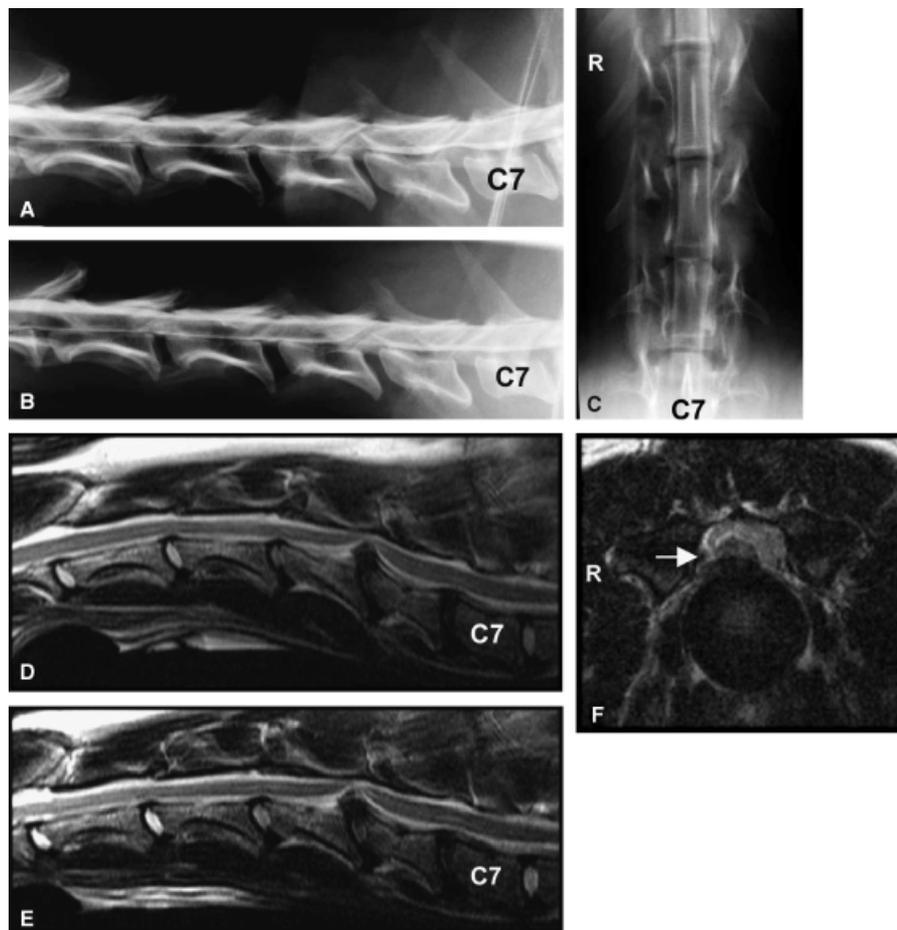
FIG. 3. Cervical myelogram and T2-weighted images of a 9-year-old, female spayed Doberman pinscher dog with severe ataxia (grade 4). (A) Pretraction cervical myelogram. There is ventral extradural spinal cord compression at C6–7 and splitting of the ventral aspect of the contrast medium column at C5–6. (B) Posttraction cervical myelogram. There is improvement in the spinal cord compression and in the splitting of the contrast medium. Two reviewers classified these lesions as static, with a dynamic component, and another reviewer classified as dynamic. (C) Ventrodorsal myelogram. There is bilateral widening of the contrast medium column at C5–6. No asymmetric compression is seen. (D) Pretraction sagittal T2-weighted image. There is marked spinal cord compression at C5–6, with minimal spinal cord compression at C6–7. Intervertebral disc degeneration is observed at C4–5, C5–6, and C–7. (E) Posttraction sagittal T2-weighted image. There is still marked spinal cord compression at C5–6. All reviewers classified this lesion as static. (F) Transverse T2-weighted image. Note the markedly asymmetric spinal cord compression, worse on the right side, caused by a hypointense region in the ventral aspect of the vertebral canal (arrow). C7, seventh cervical vertebrae.

Fourteen dogs (77%) had foraminal stenosis, classified as mild in six dogs, moderate in four dogs, and severe in four dogs. The foramina at C6–7 were affected in 12 dogs, followed by C5–6 (11 dogs). All dogs with severe foraminal stenosis had spinal cord signal changes.

Vertebral body tipping or tilting was observed in seven out of 18 dogs (39%). It affected the sixth cervical vertebrae in all dogs. In three of these dogs, the tipping worsened upon traction. Spondylosis was observed at C6–7 in four dogs and at C7–T1 in one dog.

Discussion

In this study, MR imaging was effective in localizing the site of spinal cord compression at a different place than indicated on myelography in two dogs, in revealing the severity of spinal cord involvement in two other dogs, and in identifying the probable cause of the clinical signs when myelography was normal in one additional dog. All three reviewers had 100% agreement on the site of lesion using MR imaging, whereas discrepancies existed using myelography. A distinct advantage of MR imaging is the ability to assess the spinal cord parenchyma, while on myelography, only the spinal cord contour is seen. This advantage allowed visualization of signal changes in the spinal cord parenchyma and precise lesion localization.

In the present investigation, 10 out of 18 dogs (55%) had spinal cord signal changes, significantly higher than previously reported in dogs with cervical spondylomyelopathy (three out of 21 dogs).[26] Signal changes within the spinal cord are a common and important MR imaging feature of cervical spondylotic myelopathy in humans. Proposed causes include direct spinal cord compression and ischemia.[27]

Although spinal cord compression seems the most likely cause in our dogs, all dogs with severe foraminal stenosis also showed spinal cord signal changes; however, these dogs also showed spinal cord compression.

In humans, the correlation between spinal cord signal changes seen with MR imaging and histopathologic appearance of the spinal cord has been documented.[28] Areas of hyperintensity in T2-weighted images without changes in T1 images were characterized histologically by slight loss of nerve cells, gliosis, and edema in the gray matter, as well as demyelination, edema, and Wallerian degeneration in the white matter. Again, in humans, the combination of T2 hyperintensity and T1 hypointensity was characterized by severe histologic changes such as necrosis, myelomalacia, and spongiform changes in the gray matter, as well as white matter necrosis.[28] There are no studies relating the spinal cord signal changes seen on MR images with histopathologic appearance in dogs with cervical spondylomyelopathy. However, in a canine model of chronic cervical myelopathy, MR imaging changes in spinal cord corresponded histologically to motor neuron loss, gray matter necrosis, and cavitation.[29] It was recently proposed that hyperintensity in the T2-weighted images seen in humans with cervical spondylotic myelopathy likely reflects pathologically reversible changes, while the combination of hyperintensity in T2-weighted images and hypointensity in T1-weighted images suggests irreversible spinal cord changes and a poorer prognosis.[30,31] In dogs, spinal cord T2 hyperintensity seen with acute spinal cord compression caused by intervertebral disc disease was a more accurate predictor of poor outcome than loss of deep pain perception.[32] However, at this time the clinical and prognostic significance of such spinal cord signal changes in cervical spondylomyelopathy is not known.

In our study spinal cord signal changes seemed to be associated with severity of clinical signs, as 75% of dogs with moderate and severe ataxia, and the nonambulatory dog had signal changes. Spinal cord signal changes were not seen in dogs with cervical hyperesthesia or mild ataxia. Spinal cord signal changes were not present in 16 clinically normal Doberman pinschers, even though some had spinal cord compression.[33] The duration of clinical signs also seemed to be related to spinal cord signal changes, since all dogs with a chronic history had such changes. On the other hand, two out of three dogs with moderate or severe ataxia but acute presentation did not have signal changes within the spinal cord. This observation agrees with studies in humans, suggesting that the spinal cord signal changes seen in cervical spondylomyelopathy are usually associated with chronic evolution of signs.[27] However, acute spinal cord trauma has also been shown to produce spinal cord signal changes in dogs and cats.[34,35]

The classification of lesions as static or dynamic is problematic. We observed disagreement in the classification of lesions as static or dynamic between myelography and MR imaging and also among reviewers. Depending on the reviewer, two to four dogs had the lesions classified as dynamic on myelography, but as static on MR imaging. Overall, most dogs had lesions classified as static. The reviewers disagreed upon the type of lesion in 44% of dogs using myelography and 33% of dogs using MR imaging. The high disagreement reflects the lack of criteria to determine whether a lesion is static or dynamic. This has also been noted in 28 Dobermans with cervical spondylomyelopathy imaged using myelography.[36] In that study, all 14 dogs evaluated by neurologists were considered to have static lesions, while all 14 evaluated by surgeons were assumed to have dynamic lesions.[36] It is possible, although unlikely, that the body position used for myelography vs. MR imaging could partially account for these differences.

The concept of static and dynamic lesions was first established in 1982.[9] Lesions that improved or disappeared upon traction or flexion/extension views were considered dynamic. Owing to the risk of neurologic deterioration after these cervical manipulations, only traction positions continue to be routinely used.[1] The technique of traction was rather subjective as it was described as grasping the dog behind the base of the skull while applying firm linear traction.[9] Based on this concept, a multitude of surgical techniques were developed for the treatment of dynamic lesions.[3,6,24,37–39] It was never established how much traction should be used and how it should be performed. The myelographic findings can also be misleading in defining whether a lesion is static or dynamic. The dog in Fig. 2 illustrates this problem. It must be remembered that the dura mater and the spinal cord have elastic properties to adjust themselves to changes in neck position according to movement. In a traction study in normal cats, it was demonstrated that the caudal cervical region has significantly higher vertebral and spinal cord motion compared with the cranial cervical spine.[40] It has also recently been shown that the amount of intervertebral disc distraction is similar between clinically normal Doberman pinschers and Dobermans with cervical spondylomyelopathy.[33] Because of the inherent elastic properties of the cervical spine and the fact that it is only possible to visualize the contrast medium column on myelography, it is possible that any lesion would improve under traction, even though it would in fact be a static lesion. This concept is illustrated in Fig. 3.

The technique and ideal amount of traction of the cervical spine have never been evaluated objectively. In our pilot experiments, it appeared that 20% of the dog's weight was enough to produce sufficient traction. In humans, traction studies were performed with approximately 20% to 30% of the patient's body weight, recommending not exceeding 33%.[13,41] These recommendations were based on nonanesthetized human patients. In an anesthetized dog, muscle tone would not counteract the traction force;

therefore, less traction would likely be needed to produce the same degree of spinal distraction as in humans. Experimentally, excessive distraction can cause ischemia and disruption of the spinal cord interstitial pressure with permanent spinal cord damage.[42,43] Based on the above considerations, the authors believe that it is unnecessary to use traction forces higher than 25% of the patient's weight. However, further studies are needed to establish the distraction efficacy of the different weights, traction methods, and the necessity and safety associated with the procedure.

The MR imaging protocol used in this study was time consuming. We chose this protocol to evaluate precisely all structures affected in cervical spondylomyelopathy. In humans, foraminal stenosis is one of the key factors in the pathogenesis of cervical spondylotic myelopathy, causing or contributing to spinal cord ischemia.[44,45] The magnitude of its importance in humans led us to include specifically a gradient echo FLASH sequence associated with MT, and pre and postintravenous gadolinium images for assessment of intervertebral foramina. In humans, the FLASH sequence with MT provided the best anatomic detail for the cervical spinal cord, intervertebral foramina, cerebrospinal fluid, and compact bone, compared with other sequences.[46,47] When contrast enhancement was combined with MT, it improved the assessment of the intervertebral foramina avoiding overestimation of foraminal stenosis.[48] It is our impression that there was no significant difference between the images with and without gadolinium; therefore, only one sequence needs to be used in the clinical setting. In agreement with the findings in humans, the FLASH-MT-weighted images were clearly superior with regard to visualization of the intervertebral foramina compared with conventional T2- and T1-weighted images. Using the FLASH-MT images, we found foraminal stenosis in 77% of dogs. The clinical significance of this finding needs to be clarified further, as in a recent study 69% of 16 clinically normal Dobermans also had foraminal stenosis.[33]

In summary, we documented that MR imaging allows identification of more abnormalities than cervical myelography in Dobermans pinscher dogs with cervical spondylomyelopathy. Although myelography could identify the location of the lesion in most patients, MR imaging was more accurate in predicting the site, severity, and nature of spinal cord compression. Also, spinal cord signal changes were seen in the majority of patients. The distinction between dynamic and static lesions is currently unclear, subjective, and dependent on personal opinion. Most static lesions can apparently have a dynamic component upon traction myelography. If we are to evolve in the diagnosis and treatment of cervical spondylomyelopathy, further studies are needed to establish guidelines in performing and interpreting the findings of kinematic imaging tests, as well as determining the clinical and prognostic significance of signal changes within the spinal cord.

REFERENCES

1. Sharp NJH, Wheeler SJ, Cofone M. Radiological evaluation of 'wobbler' syndrome—caudal cervical spondylomyelopathy. J Small Anim Pract 1992;33:491–499.

2. Lewis DG. Cervical spondylomyelopathy ('wobbler' syndrome) in the dog: a study based on 224 cases. J Small Anim Pract 1989;30:657–665.

3. VanGundy TE. Disc-associated wobbler syndrome in the Doberman pinscher. Vet Clin North Am Small Anim Pract 1988;18:667–696.

4. McKee WM, Sharp NJH. Cervical spondylopathy. In: Slatter DH (ed): Textbook of small animal surgery, 3rd ed. Philadelphia: Saunders, 2003;1180–1193.

5. Chrisman CL, Mariani C, Platt S, Clemmons R. Ataxia. In: Chrisman CL, Mariani C, Platt S, Clemmons R (eds): Neurology for the small animal practitioner. Jackson: Teton New Media, 2003;207–210.

6. Sharp NJH, Wheeler SJ. Cervical spondylomyelopathy. In: Sharp NJH, Wheeler SJ (eds): Small animal spinal disorders diagnosis and surgery, 2nd ed. Philadelphia: Elsevier Mosby, 2005;211–246.

7. Batzdorf U, Flannigan BD. Surgical decompressive procedures for cervical spondylotic myelopathy. A study using magnetic resonance imaging. Spine 1991;16:123–127.

8. Smith JK, Castillo M. New sequences for Spinal MR imaging: basic concepts. In: Castillo M (ed): Spinal imaging state of the art, 1st ed. Philadelphia: Hanley & Belfus Inc, 2001;1–16.

9. Seim HB, Withrow SJ. Pathophysiology and diagnosis of caudal cervical spondylo-myelopathy with emphasis on the Doberman Pinscher. J Am Anim Hosp Assoc 1982;18:241–251.

10. Penderis J, Dennis R. Use of traction during magnetic resonance imaging of caudal cervical spondylomyelopathy ("wobbler syndrome") in the dog. Vet Radiol Ultrasound 2004;45:216–219.

11. Muhle C, Weinert D, Falliner A, et al. Dynamic changes of the spinal canal in patients with cervical spondylosis at flexion and extension using magnetic resonance imaging. Invest Radiol 1998;33:444–449.

12. Muhle C, Metzner J, Weinert D, et al. Kinematic MR imaging in surgical management of cervical disc disease, spondylosis and spondylotic myelopathy. Acta Radiol 1999;40:146–153.

13. Chung TS, Lee YJ, Kang SW, Park CJ, Kang WS, Shim YW. Reducibility of cervical disk herniation: evaluation at MR imaging during cervical traction with a nonmagnetic traction device. Radiology 2002;225:895–900.

14. Masaryk TJ, Modic MT, Geisinger MA, et al. Cervical myelopathy: a comparison of magnetic resonance and myelography. J Comput Assist Tomograph 1986;10:184–194.

15. Modic MT, Masaryk TJ, Mulopulos GP, Bundschuh C, Han JS, Bohlman H. Cervical radiculopathy: prospective evaluation with surface coil MR imaging, CT with metrizamide, and metrizamide myelography. Radiology 1986;161:753–759.

16. Modic MT, Ross JS, Masaryk TJ. Imaging of degenerative disease of the cervical spine. Clin Orthop Relat Res 1989;239:109–120.

17. Larsson EM, Holtas S, Cronqvist S, Brandt L. Comparison of myelography, CT myelography and magnetic resonance imaging in cervical spondylosis and disk herniation. Pre- and postoperative findings. Acta Radiol 1989;30:233–239.

18. Nagata K, Kiyonaga K, Ohashi T, Sagara M, Miyazaki S, Inoue A. Clinical value of magnetic resonance imaging for cervical myelopathy. Spine 1990;15:1088–1096.

19. Jia LS, Shi ZR. MRI and myelography in the diagnosis of lumbar canal stenosis and disc herniation. A comparative study. Chin Med J (England) 1991;104:303–306.

20. Neuhold A, Stiskal M, Platzer C, Pernecky G, Brainin M. Combined use of spin-echo and gradient-echo MR-imaging in cervical disk disease. Comparison with myelography and intraoperative findings. Neuroradiology 1991;33:422–426.

21. Perneczky G, Bock FW, Neuhold A, Stiskal M. Diagnosis of cervical disc disease. MRI versus cervical myelography. Acta Neurochir (Wien) 1992;116:44–48.

22. Bischoff RJ, Rodriguez RP, Gupta K, Righi A, Dalton JE, Whitecloud TS. A comparison of computed tomography-myelography, magnetic resonance imaging, and myelography in the diagnosis of herniated nucleus pulposus and spinal stenosis. J Spinal Disord 1993;6: 289–295.

23. Reul J, Gievers B, Weis J, Thron A. Assessment of the narrow cervical spinal canal: a prospective comparison of MRI, myelography and CT-myelography. Neuroradiology 1995;37:187–191.

24. McKee WM, Butterworth SJ, Scott HW. Management of cervical spondylopathy-associated intervertebral disc protrusions using metal washers in 78 dogs. J Small Anim Pract 1999;40:465–472.

25. Landis JR, Koch GG. The measurement of observer agreement for categorical data. Biometrics 1977;33:159–174.

26. Lipsitz D, Levitski RE, Chauvet AE, Berry WL. Magnetic resonance imaging features of cervical stenotic myelopathy in 21 dogs. Vet Radiol Ultrasound 2001;42:20–27.

27. Takahashi M, Yamashita Y, Sakamoto Y, Kojima R. Chronic cervical cord compression: clinical significance of increased signal intensity on MR images. Radiology 1989;173:219–224.

28. Ohshio I, Hatayama A, Kaneda K, Takahara M, Nagashima K. Correlation between histopathologic features and magnetic resonance images of spinal cord lesions. Spine 1993;18:1140–1149.

29. al-Mefty O, Harkey HL, Marawi I, et al. Experimental chronic compressive cervical myelopathy. J Neurosurg 1993;79:550–561.

30. Suri A, Chabbra RP, Mehta VS, Gaikwad S, Pandey RM. Effect of intramedullary signal changes on the surgical outcome of patients with cervical spondylotic myelopathy. Spine J 2003;3:33–45.

31. Morio Y, Teshima R, Nagashima H, Nawata K, Yamasaki D, Nanjo Y. Correlation between operative outcomes of cervical compression myelopathy and MRI of the spinal cord. Spine 2001;26: 1238–1245.

32. Ito D, Matsunaga S, Jeffery ND, et al. Prognostic value of magnetic resonance imaging in dogs with paraplegia caused by thoracolumbar intervertebral disk extrusion: 77 cases (2000–2003). J Am Vet Med Assoc 2005;227:1454–1460.

33. da Costa RC, Parent JM, Partlow G, Dobson H, Holmberg D, LaMarre J. Morphologic and morphometric magnetic resonance imaging features of Doberman pinscher dogs with and without clinical signs of cervical spondylomyelopathy. Am J Vet Res 2006;67:1601–1612.

34. Schouman-Claeys E, Frija G, Cuenod CA, Begon D, Paraire F, Martin V. MR imaging of acute spinal cord injury: results of an experimental study in dogs. Am J Neuroradiol 1990;11:959–965.

35. Takahashi T, Suto Y, Kato S, Ohama E. Experimental acute dorsal compression of cat spinal cord: correlation of magnetic resonance signal intensity with spinal cord evoked potentials and morphology. Spine 1996;21:166–173.

36. Rusbridge C, Wheeler SJ, Torrington AM, Pead MJ, Carmichael S. Comparison of two surgical techniques for the management of cervical spondylomyelopathy in dobermanns. J Small Anim Pract 1998;39:425–431.

37. Ellison GW, Seim HB, Clemmons RM. Distracted cervical spinal fusion for management of caudal cervical spondylomyelopathy in large-breed dogs. J Am Vet Med Assoc 1988;193:447–453.

38. Dixon BC, Tomlinson JL, Kraus KH. Modified distraction-stabilization technique using an interbody polymethyl methacrylate plug in dogs with caudal cervical spondylomyelopathy. J Am Vet Med Assoc 1996;208:61–68.

39. Jeffery ND, McKee WM. Surgery for disc-associated wobbler syndrome in the dog- an examination of the controversy. J Small Anim Pract 2001;42:574–581.

40. Maiman DJ, Coats J, Myklebust JB. Cord/spine motion in experimental spinal cord injury. J Spinal Disord 1989;2:14–19.

41. Panjabi MM, Yue JJ, Dvorak J, Goel V, Fairchild TA, White AA. Cervical Spine Kinematics and Clinical Instability. In: The Cervical Spine Research Society (ed): The cervical spine, 4th ed. Philadelphia: Lippincott Williams & Wilkins, 2005;55–78.

42. Jarzem PF, Kostuik JP, Filiaggi M, Doyle DJ, Ethier R, Tator CH. Spinal cord distraction: an in vitro study of length, tension, and tissue pressure. J Spinal Disord 1991;4:177–182.

43. Jarzem PF, Quance DR, Doyle DJ, Begin LR, Kostuik JP. Spinal cord tissue pressure during spinal cord distraction in dogs. Spine 1992;17: S227–S234.

44. Parke WW. Correlative anatomy of cervical spondylotic myelopathy. Spine 1988;13:831–837.

45. Fehlings MG, Skaf G. A review of the pathophysiology of cervical spondylotic myelopathy with insights for potential novel mechanisms drawn from traumatic spinal cord injury. Spine 1998;23:2730–2737.

46. Held P, Seitz J, Frund R, Nitz W, Lenhart M, Geissler A. Comparison of two-dimensional gradient echo, turbo spin echo and two-dimensional turbo gradient spin echo sequences in MRI of the cervical spinal cord anatomy. Eur J Radiol 2001;38:64–71.

47. Finelli DA, Hurst GC, Karaman BA, Simon JE, Duerk JL, Bellon EM. Use of magnetization transfer for improved contrast on gradient-echo MR images of the cervical spine. Radiology 1994;193:165–171.

48. Melhem ER, Bert RJ, Faddoul SG. Cervical spondylosis: contrast-enhanced magnetization transfer prepulsed 3D turbo field echo MR imaging. J Magn Reson Imaging 2000;11:294–298.